◆ Human Brain Mapping 8:73–79(1999) ◆

Creation and Use of a Talairach-Compatible Atlas for Accurate, Automated, Nonlinear Intersubject Registration, and Analysis of Functional Imaging Data

Roger P. Woods,[1]* Mirella Dapretto,[1] Nancy L. Sicotte,[1] Arthur W. Toga,[1,2] and John C. Mazziotta[1,3]

[1]*Division of Brain Mapping, Department of Neurology, Neuropsychiatric Institute, UCLA School of Medicine, Los Angeles, California*
[2]*Laboratory of Neuro Imaging, Neuropsychiatric Institute, UCLA School of Medicine, Los Angeles, California*
[3]*Departments of Pharmacology and Radiology, Neuropsychiatric Institute, UCLA School of Medicine, Los Angeles, California*

Abstract: Spatial normalization in functional imaging can encompass various processes, including nonlinear warping to correct for intersubject differences, linear transformations to correct for identifiable head movements, and data detrending to remove residual motion correlated artifacts. We describe the use of AIR to create a custom, site-specific, normal averaged brain atlas that can be used to map T2 weighted echo-planar images and coplanar functional images directly into a Talairach-compatible space. We also discuss extraction of characteristic descriptors from sets of linear transformation matrices describing head movements in a functional imaging series. Scores for these descriptors, derived using principal components analysis with singular value decomposition, can be treated as confounds associated with each individual image in the series and systematically removed prior to voxel-by-voxel statistical analysis. *Hum. Brain Mapping 8:73–78, 1999.*

Key words: stereotaxis; fMRI; PET; statistics; brain atlas

INTRODUCTION

The ability to map functional imaging data from different subjects into a common anatomic frame of reference has become an indispensable aspect of analysis and reporting of human brain mapping data. Despite well-documented imperfections in fully accounting for anatomic differences between subjects, the ability of even simple linear transformations to improve statistical power, to allow results to be generalized from individuals to populations, and to facilitate communication of anatomic locations between

Contract grant sponsor: National Institute of Neurological Disorders and Stroke; Contract grant number: 1 K08 NS-01646; Contract grant sponsor: NCRR; Contract grant numbers: RR05956; RR13642; Contract grant sponsor: NSF; Contract grant number: DBI 9601356; Contract grant sponsor: Human Brain Project; Contract grant number: MH/DA52176.

*Correspondence to: Roger P. Woods, M.D., Ahmanson-Lovelace Brain Mapping Center, Division of Brain Mapping and Department of Neurology, Neuropsychiatric Institute, UCLA School of Medicine, Los Angeles, CA 90095-7085. Email: rwoods@ucla.edu

Received for publication 6 April 1999; accepted 16 June 1999

laboratories has been established with certainty. In this context, continued validation and improvement in methods for mapping data into a common space is of major importance.

For functional imaging studies that seek to make inferences about groups or populations, the issue of anatomic standardization arises in two fairly different contexts. The first of these is the context of correcting for changes in head position within each individual subject. To a large extent, these corrections can proceed with considerable accuracy on the assumption that the head acts as a rigid body that is merely rotated and translated in space. A variety of methods can be used to estimate these movements, and the data can be corrected posthoc to compensate for a substantial amount of the error that such movements produce. However, interpolation errors will generally persist under even the best of circumstances, and movements at certain frequencies can interact with the physics and temporal dynamics of image acquisition protocols to produce artifacts that are difficult to model and correct on the basis of first principles.

The other context in which anatomic standardization arises in functional imaging is the correction of anatomic differences between subjects. This context is considerably more complex because the processes that govern brain development are not constrained by mathematical equations or simple physical principles, but rather are dictated by complex interactions of genes and the environment. The notion that some straightforward mathematical equation derived a priori might have special validity for mapping one person's brain onto the brain of another is implausible in view of our current understanding of brain development. Indeed, even the notion that it is possible to map one brain onto another in some uniquely appropriate manner is unlikely. For example, it has become clear that homologies based on sulcal and gyral landmarks can conflict with homologies based on cytoarchitectonic boundaries. Any mapping from one individual to another is guaranteed to be only an approximation since different criteria are often mutually contradictory.

The challenge faced when attempting to analyze functional imaging data is, therefore, largely a challenge of underconstraint with respect to anatomic standardization. On an individual basis, rigid body assumptions constrain the spatial transformation model, but interactions between the underlying movements and signal collection and interpolation result in intensity variations that need to be modeled empirically. Across subjects, it is the spatial transformation itself that can be approximated only by some mathematical model that is typically far more constrained than the underlying developmental processes. New methods for improving the modeling of these factors requires validation that recognizes their underconstrained nature and provides a pragmatic sense of their utility. We have recently described detailed validations of automated methods for registering images both within and across subjects [Woods et al., 1998a, b]. Here, we detail the application and extension of these methods to the specific problem of analysis of functional imaging data.

MATERIALS AND METHODS

T1 and T2 EPI image acquisition

All data were collected in accordance with protocols approved by the UCLA Human Subject Research Protection Committee. Ten normal subjects recruited at UCLA as part of the Human Brain Project International Consortium for Brain Mapping (ICBM) were identified and used to create conventional T1 and echo-planar T2 weighted average brain atlases. Subjects were aged 18–40 years and had normal neurologic examinations. All images were acquired on a 3 Tesla GE MRI scanner equipped with ANMR (Willmington, MA) echo-planar imaging (EPI) capabilities. The T1 weighted images were acquired as 1 NEX 3D spoiled grass images with TR = 24 msec and TE = 4 msec and a field of view of 250 mm by 250 mm by 150 mm. The echo-planar T2 weighted images were collected with TE = 65 msec, TR = 4,000 msec 4 NEX, 128 × 128 matrix with a 20 cm field of view and 26–27 interleaved 4 mm slices with 1 mm gaps between slices, parameters that reproduce a protocol routinely used at our center for routine fMRI studies. A subset of these T2 image slices is subsequently used for acquisition of coplanar functional data in fMRI studies.

T1 atlas

The T1 images for each subject were manually edited to remove the scalp, skull, and dura. These images from different subjects were then aligned to one another using the same general strategy that has been previously described [Woods et al., 1998a, b]. This strategy began with pairwise affine registration of each subject to all other subjects and reconciliation of internal inconsistencies among these pairs before creation of an initial affine average atlas. Three additional intermediate linear atlases were created iteratively by registering each of the original 10 T1 weighted images to the current averaged atlas. Transformation matrix

averaging techniques were used to assure that the size and affine shape of the averaged atlases reflected the average size and affine shape of the original 10 subjects. Three further iterations allowed for nonlinear warping in registration of the individual T1 weighted images to the current intermediate averaged atlas.

The nonlinear warping methods have been described previously [Woods et al., 1998b], but were extended here to allow polynomial transformations as high as eighth order (495 independent parameters). The top of the anterior commissure and the bottom of the posterior commissure was identified in each of the original T1 weighted images and the coordinate location of these two landmarks was mapped into the third nonlinear intermediate averaged atlas using the fitted registration parameters. The coordinate locations for all 10 anterior commissures were then averaged to identify the mean location of this landmark in the third nonlinear intermediate averaged atlas. The posterior commissures were mapped similarly. The third nonlinear averaged atlas was then recreated with application of a rigid body transformation that would place the average anterior and posterior commissures and the midsagittal plane into the orientation specified by Talairach et al. [1967] and Talairach and Tournoux [1988]. Finally, scaling factors along the three cardinal axes were computed sufficient to match the extent of the brain along each of these axes to the corresponding dimension in the 1988 Talairach atlas. These scaling factors were mathematically combined with all previous linear and nonlinear transformations and used to resample each original T1 weighted image into a Talairach compatible frame of reference. These resampled images were then averaged to create a final T1 weighted atlas. From the standpoint of which points were treated as homologous across subjects, this atlas was identical to the third nonlinear intermediate averaged atlas.

T2 EPI atlas

Each T2 weighted echo-planar image was registered to the corresponding original T1 weighted image from the same subject [Woods et al., 1993], and this transformation was combined mathematically with the transformation need to map the T1 image into the final T1 atlas. All registrations of the T2 images to the T1 images were inspected manually to assure that the geometric and susceptibility artifacts associated with high field strength echo-planar imaging did not disrupt the registration. This combined transformation was then used to resample each original, unedited T2 weighted image into the same space as the final T1 weighted atlas. The 10 transformed T2 weighted images were then averaged together to create a final nonlinear T2 EPI averaged atlas. Further adjustments to the transformation parameters allowed creation of a version of this T2 EPI averaged atlas and the T1 averaged atlas with voxel sizes and file dimensions compatible with SPM96. This T2 EPI averaged atlas has subsequently been routinely used at UCLA as a template for spatial normalization of newly acquired T2 echo-planar images using nonlinear transformations derived using AIR. After spatial normalization and removal of motion correlated artifacts (described in the next section), the data are of appropriate dimensions for routine statistical analysis with SPM. Since the T1 and T2 atlases are based on matched data sets, the T1 averaged atlas also can be used for data display within SPM96, using either sectional data from the averaged atlas itself or 3D renderings of spatially normalized T1 data from a representative subject chosen at random.

Removal of motion correlated artifacts

The target atlases described above allow data from different subjects to be mapped into a common space. A more constrained affine spatial transformation is also used to correct for head movements within each individual subject using methods described previously [Woods et al., 1998a]. However, even perfect registration does not fully eliminate motion correlated artifacts that can confound data analysis. Within each run of functional data, it is possible to derive a series of linear transformations that describes the movements from one scan to the next. Due to physical constraints (e.g., the fact that the back of the head generally remains in contact with the scanner bed), certain types of rotations and translations are likely to be correlated with one another. To develop optimal descriptors of head movements for the purpose of estimating the artifacts induced by such movements, we use a form of principal components analysis to extract and quantify eigenmovements that characterize each data acquisition. This is accomplished by defining an average position for each run such that the matrix logarithm of the deviation of each individual position from the average sums across all images to a matrix of zeros. Principal component analysis can then be applied to the 12 elements of the matrices that describe deviations from this average position for each individual image in the run.

If desired, the eigenvectors produced by the PCA can be placed back into matrix format and exponentiated to derive corresponding eigenmovements, but

more importantly, the scores associated with each individual image for a given eigenmovement quantify the amount of that eigenmovement present at the time that image was acquired. If the images are registered to one another with a six parameter rigid body spatial transformation model, only the first six scores will be significant and the other six will be negligibly small. In theory, it is possible that the six eigenmovements might correspond to traditional elemental movements such as pitch, roll, yaw, x-translation, y-translation, and z-translation, but in practice, they will generally be hybrid movements incorporating various orthogonal (in the matrix logarithm sense) mixtures of these elemental movements.

To look for motion-correlated artifacts in motion-corrected data sets, we perform principal components analysis of the functional imaging data after motion correction has been applied. This produces eigenimages and corresponding scores for each of the original images in the series. A strong correlation between the scores that relate to the eigenimages and the scores that quantify the eigenmovements is indicative of residual motion correlated artifacts. Such correlations can be eliminated from the data on a voxel-by-voxel basis by treating the scores for each eigenmovement as a linear confounds to be removed using standard linear algebraic techniques. For fMRI time series with large numbers of observations across time, all six sets of scores can be removed with limited impact on the statistical properties of the adjusted data. For PET data where the total number of observations per subject is much smaller, confound removal can be restricted to those eigenmovements that account for the greatest amount of the total movement present in the data. Particularly in this latter case, it is appropriate to adjust the number of degrees of freedom in any subsequent statistical analysis to reflect the fact that additional parameters have been added to the data analysis model.

Representative fMRI time series

A representative covert language task fMRI time series was acquired with an EPI gradient echo sequence (TR = 2,500 msec, TE = 45 msec, matrix size 64 × 64, FOV = 20 cm). The images were registered to the first image in the series using AIR 3.0 with a rigid body spatial transformation model. The images were then resampled to create a motion-corrected time series using chirp z interpolation [Rabiner et al., 1969] within plane and linear interpolation between planes. Chirp z interpolation is a Fourier domain analogue of sinc interpolation. The transformation matrices were subjected to principal components analysis for eigenmovements using singular value decomposition of the elements of the matrix logarithm of the deviation of each position from the mean position. The motion-corrected time series was subjected to principal components analysis to create eigenimages and scores for each individual time point in the fMRI series. Only brain regions where data were available throughout the entire time series were included in the PCA.

RESULTS

Figure 1 shows sections through the final T1 and T2 echo-planar atlases and illustrates the excellent level of anatomic detail that is preserved by the high-order polynomial warping used to create the atlases. Although the individual echo-planar images showed distortions relative to the T1 images, the amount of mismatch was small compared to the amount of intersubject variability routinely encountered with this and other low-order registration methods.

Figure 2 shows the scores for the first principal eigenmovement in the motion-corrected fMRI time series and the scores for the first principal eigenimage of the same motion-corrected data before removal of any movement related confounds. Figure 3 shows the results of two different SPM analyses conducted on data from a single subject (top panel) and from a group of eight subjects (bottom panel) with and without removal of motion correlated artifacts.

DISCUSSION

With acquisitions that are nominally "T1 weighted" or "T2 weighted," different scanners can produce data sets that are dissimilar even to visual inspection. Given that the sensitivity of intensity based registration algorithms to such dissimilarity has not been well characterized, the use of atlas templates generated using the same scanner as the data of interest assures that registration accuracy is optimized. Our efforts to create the atlas described here stemmed largely from substantial difficulties encountered when trying to register T2 weighted anatomic images from our scanner to atlases created on other scanners. The benefits of our custommade atlas have been evident with simple visual inspection of typical data sets. Although we have not yet performed a detailed validation of the anatomic accuracy of this approach with T2 weighted echo-planar data, extensive validation with T1 weighted data has demonstrated highly accurate mapping of homologous landmarks to similar locations in the atlas [Woods et al., 1998b]. An argument could be

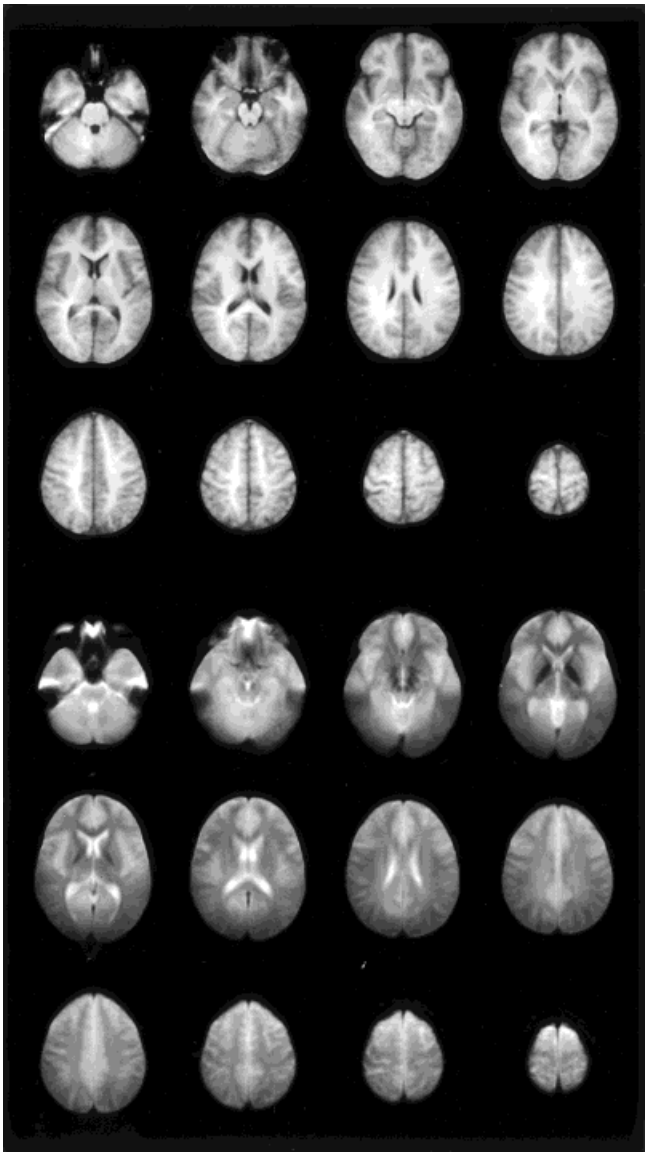

Figure 1.
Transverse sections through the T1 (top) and T2 EPI (bottom) atlases. Note the preservation of anatomic features despite the fact that the images are intensity averages of 10 different subjects.

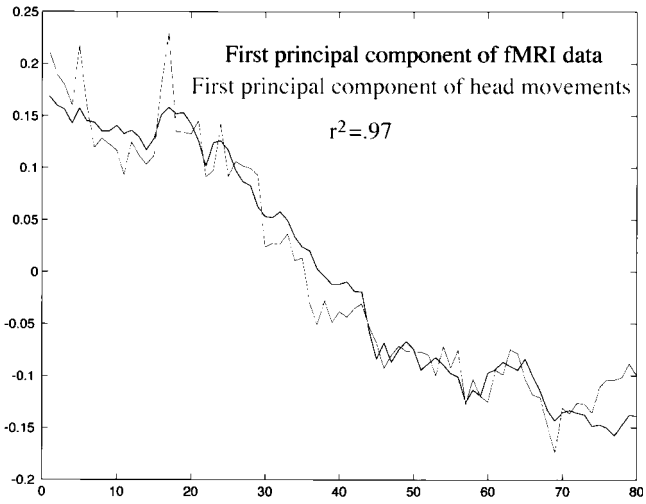

Figure 2.
Motion-correlated artifacts in a typical fMRI time series. Each individual image in the time series is represented along the x-axis. The values on the y-axis are principal components analysis scores. The darker line shows scores from the first principal component of a traditional PCA of the motion-corrected images. The lighter line shows the first principal component from a PCA of the linear transformations representing the head movements. The values are highly correlated, indicating the persistence of motion-correlated artifacts despite motion correction of the data. After adjustment of the fMRI time series data using the scores from the first principal component of the head movements to remove this confound, the largest principal component of the adjusted data was correlated with scores from the second principal component of the head movements ($r^2 = .72$). Treatment of scores from the first two principal components of the head movements as confounds resulted in corrected image data with first principal component that was correlated with the third principal component of the head movements ($r^2 = .76$).

made in favor of always acquiring T1 weighted data for the purpose of registration to a T1 atlas, but time constraints during image acquisition strongly favor the use of the T2 echo-planar images. By acquiring images with greater brain coverage than is planned for the fMRI data itself, the registration problem can be more accurately constrained. The fMRI data can then be acquired co-planar to a subset of the anatomic T2 images. On occasions when a subject moves between the acquisition of the T2 echo-planar image and the first fMRI image, image registration between the mean registered fMRI image and the T2 echo-planar image allows accurate mappings to be created.

Simple interpolative resampling of the images to correct for movement does not remove all of the motion-correlated artifacts, and our experience to date indicates that motion correlated artifact is commonly the greatest source of global variance in the motion corrected data set. It should be noted that the global variance as identified by principal components analysis may be particularly sensitive to motion-correlated artifacts because they are likely to occur throughout the entirety of the image. As a result, the contribution at any particular voxel may be small despite a very large global contribution. We suspect that interpolation artifacts are a major contributor to these errors, but note that the mathematical form of our correction

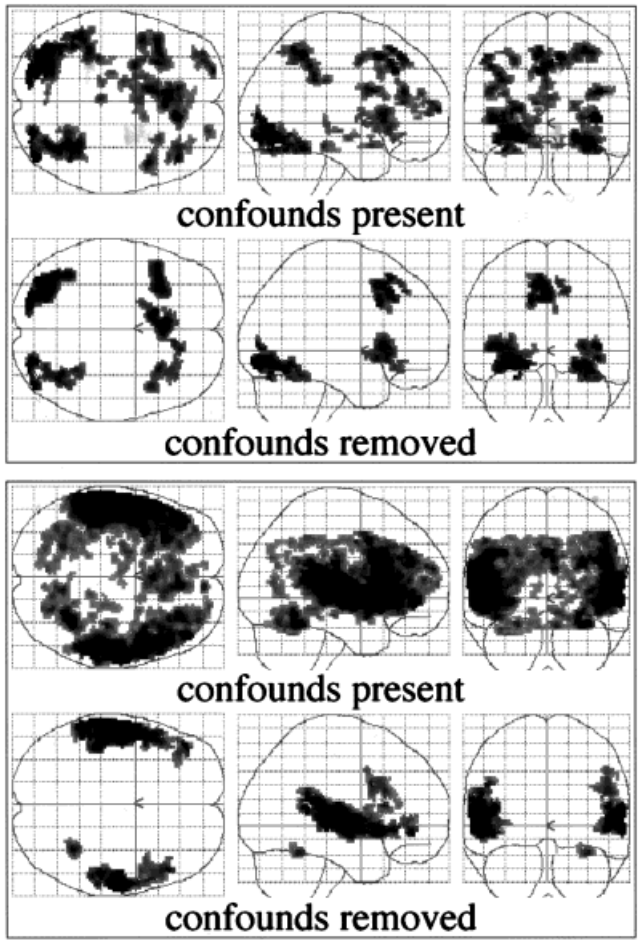

Figure 3.

Statistical parametric maps of analyses conducted on data from a single subject (top panel) performing a picture-word matching task and from a group of eight subjects (bottom panel) during an auditory sentence-judgement task. Note the reduction of diffuse signals and preservation of focal activations after removal of motion-correlated signals in both data sets. For each data set, the statistical thresholds applied were identical for the data with and without removal of motion-correlated confounds.

is identical to the linear correction terms used by Friston et al. [1996] for ''spin-history correction'' of fMRI data. From a pragmatic standpoint, the source of the error is not particularly important unless this information can be used to provide more appropriate corrections than those derived empirically by removal of confounds. Our use of principal components analysis to extract scores for eigenmovements offers certain theoretical advantages over the direct use of the unprocessed registration parameters. Since we measure deviations from a mathematically defined mean position, we effectively define an ideal tangent space in which nonlinear interactions among the various movement descriptors are minimized. Such methods have proved important in the broader context of morphometric analysis [Bookstein, 1996]. In addition, the opportunity to omit eigenmovement scores that account for only a small amount of total movement may be especially useful in contexts where the number of observations is small, as occurs for interpolation errors in PET data. Contrary to what is expected on the assumption that fMRI movement correlated artifacts are due to spin-history [Friston et al., 1996], we have not found the absolute value or the square of the eigenmovement scores to explain much of the residual variance in the eigenimage scores generated by PCA of the fMRI data after linear motion confounds have been removed. This may differ as a function of pulse sequence and warrants a more systematic investigation in the future.

Removal of motion-correlated signals is not without problems. In the event that motion is strongly correlated with the neurocognitive tasks being investigated, true signals may be dismissed as artifact. In this context, a better understanding of the nature of the motion-correlated signals might allow for more constrained modeling of the problem in a way that might disentangle the confounds from the true signals. In the absence of such information, investigators may want to analyze their data with and without removal of motion confounds and to make special efforts to improve their data acquisition strategies if there is a resulting concern that motion correction is eliminating genuine signal. In general, removal of motion correlated signal is likely to produce overly conservative results rather than false positives. The one possible exception is in the comparison of different groups to one another, where systematic differences in task-correlated motion between the groups may generate false signals after removal of motion-correlated confounds [Woods, 1996]. It should be possible explicitly to test for such systematic differences by analyzing head motion within the fMRI time series. If such problems are detected, new methods are being developed to take them into account statistically when performing group comparisons [Bullmore et al., 1999].

ACKNOWLEDGMENTS

We acknowledge the generous gifts from the Pierson-Lovelace Foundation, Ahmanson Foundation, Tamkin Foundation, North Star Fund, Jennifer Jones Simon Foundation, and Brain Mapping Medical Research Organization.

REFERENCES

Bookstein FL. 1996. Biometrics, biomathematics and the morphometric synthesis. Bull Math Biol 58:313–365.

Bullmore ET, Brammer MJ, Rabe-Hesketh S, Curtis VA, Morris RG, Williams SC, et al. 1999. Methods for diagnosis and treatment of stimulus-correlated motion in generic brain activation studies using fMRI. Hum Brain Mapp 7:38–48.

Friston KJ, Williams S, Howard R, Frackowiak RS, Turner R. 1996. Movement-related effects in fMRI time-series. Magn Reson Med 35:346–355.

Rabiner LR, Schafer RW, Rader CM. 1969. The chirp z-tranform algorithm and its application. Bell System Tech J 48:1249–1292.

Talairach J, Szikla G, Tournoux P, Prossalentis A, Bordas-Ferrer M, Covello L, et al. 1967. Atlas d'anatomie stéréotaxique du télencéphale. Paris: Masson.

Talairach J, Tournoux P. 1988. Co-planar Stereotaxic Atlas of the Human Brain. Stuttgart: Thieme.

Woods RP. 1996. Modeling for intergroup comparisons of imaging data. Neuroimage 4:S84–S94.

Woods RP, Grafton ST, Holmes CJ, Cherry SR, Mazziotta JC. 1998a. Automated image registration: I. General methods and intrasubject, intramodality validation. J Comput Assist Tomogr 22:139–152.

Woods RP, Grafton ST, Watson JD, Sicotte NL, Mazziotta JC. 1998b. Automated image registration: II. Intersubject validation of linear and nonlinear models. J Comput Assist Tomogr 22:153–165.

Woods RP, Mazziotta JC, Cherry SR. 1993. MRI-PET registration with automated algorithm. J Comput Assist Tomogr 17:536–546.